Geophysical Research Letters

RESEARCH LETTER
10.1029/2018GL079940

Future Changes in Seasonality of the North Pacific and North Atlantic Subtropical Highs

Fengfei Song[1], **L. Ruby Leung**[1], **Jian Lu**[1], **and Lu Dong**[1]

[1]Atmospheric Sciences and Global Change Division, Pacific Northwest National Laboratory, Richland, WA, USA

Key Points:
- Both North Pacific and North Atlantic subtropical highs are more significantly enhanced during spring than summer in response to warming
- Land-sea contrast contributes more to the enhancement in spring, but the Hadley cell dominates the seasonally dependent response
- The spring enhancement and seasonal dependence of subtropical high response have important implications for U.S. regional precipitation

Supporting Information:
- Supporting Information S1

Correspondence to:
F. Song & L. R. Leung,
fengfei.song@pnnl.gov;
ruby.leung@pnnl.gov

Citation:
Song, F., Leung, L. R., Lu, J., & Dong, L. (2018). Future changes in seasonality of the North Pacific and North Atlantic subtropical highs. *Geophysical Research Letters*, *45*, 11,959–11,968. https://doi.org/10.1029/2018GL079940

Received 6 AUG 2018
Accepted 28 SEP 2018
Accepted article online 5 OCT 2018
Published online 12 NOV 2018

Abstract The subtropical highs have a zonal mean and a zonally asymmetric component related to the Hadley cell and land-sea contrast, respectively. Based on 37 Coupled Model Intercomparison Project phase 5 models, relative roles of the Hadley cell and land-sea contrast in future changes of the North Pacific and North Atlantic subtropical highs (NPSH and NASH) are evaluated. Both the NPSH and NASH are significantly enhanced during boreal spring (April–June) but not in summer (July–September). Although the zonally asymmetric component contributes to more than half of the enhancement during spring, the zonal mean component is responsible for the interseasonal contrast of the responses of the NPSH and NASH between spring and summer. The seasonally dependent Hadley cell changes are due to changes in tropical precipitation related to sea surface temperature (SST) warming, while enhanced land-sea contrast has comparable effects on the NPSH and NASH during both spring and summer, with important implications to U.S. regional precipitation.

Plain Language Summary The North Pacific and North Atlantic subtropical highs (NPSH and NASH) are the most evident low-level atmospheric features in the Northern Hemisphere during the warm season (April–September). Both the Hadley cell and land-sea distribution contribute to its formation and seasonal variation. Previous studies only focused on the future changes of the NPSH and NASH during their peak season (June–August). Here we found that both the NPSH and NASH will be intensified more during spring (April–June) than summer (July–September) under climate warming. The enhanced land-sea thermal contrast under global warming strengthens the NPSH and NASH, with similar magnitude in spring and summer. However, the Hadley cell enhances the NPSH and NASH during spring while weakens them during summer. Hence, the seasonally dependent response of the NPSH and NASH is mainly driven by the Hadley cell. The seasonality changes of the NPSH and NASH have important implications for the U.S. regional precipitation.

1. Introduction

Subtropical highs are semipermanent lower-tropospheric features over the subtropical oceans. As fundamental elements of the global atmospheric circulations, these features have important implications to global and regional climate. Generally, the subtropical highs can be regarded as the combined contributions from the Hadley cell and land-sea contrast, which contribute to the zonal mean and zonally asymmetric components, respectively (Hoskins, 1996; Namias, 1972; Rodwell & Hoskins, 2001). In the Northern Hemisphere, the subtropical highs, known as North Pacific subtropical high (NPSH) and North Atlantic subtropical high (NASH), become strong and well organized during the warm season (April–September). As the NPSH and NASH exert large influences on the regional precipitation over East Asia and North America by modulating moisture transport (Li et al., 2011; Zhou & Yu, 2005), monsoon circulation (Chang et al., 2000; Wang et al., 2013), and tropical cyclone tracks (Colbert & Soden, 2012; Stowasser et al., 2007; Wu et al., 2005), understanding their future changes under global warming is an important scientific challenge that carries societal significance.

Previous studies on the possible changes of the NPSH and NASH have focused mainly on their peak season (June–August, He et al., 2017; Li et al., 2012; Shaw & Voigt, 2015). Li et al. (2012) found that both the NPSH and NASH will be enhanced under global warming based on CMIP3 (Coupled Model Intercomparison Project phase 3) models, but Shaw and Voigt (2015) found a large cancellation between the responses to direct radiative forcing and indirect sea surface temperature (SST) warming, and as a result, CMIP5 models projected no robust response of the NPSH in the future. These two studies only focused on the zonally asymmetric component of the NPSH and NASH. He et al. (2017) investigated the total response of the subtropical

highs to global warming and found that the NPSH will weaken, while the NASH will strengthen in the future. To date, relative contributions of the zonal mean and zonally asymmetric components to the response of the NPSH and NASH to warming have not been carefully examined. Moreover, previous studies only focused on the peak season (June–August), although the NPSH and NASH are also strong in other months (e.g., April, May, and September) of the warm season.

Recently, Song et al. (2018) found a robust seasonally dependent response of the zonal mean subtropical highs and tropical precipitation under global warming. More specifically, the subtropical highs will be strengthened more during April–June (AMJ) than July–September (JAS) in the Northern Hemisphere, accompanied by a seasonal delay of the arrival of tropical rain belt and monsoon rainfall in boreal summer. However, it is unclear whether the response of the NPSH and NASH has a similar seasonal dependence, since the contribution from the zonally asymmetric component is not known. Hence, this study focuses on the following questions: (1) What is the response of the NPSH and NASH to global warming during the whole warm season? (2) Does the response of the NPSH and NASH has a seasonal dependence? (3) What are the relative contributions of the Hadley cell and land-sea contrast to the future changes of the NPSH and NASH?

2. Model Data and Methods

Here monthly outputs of wind, sea-level pressure, precipitation, air temperature, and specific humidity from several types of CMIP5 (Table S1 in the supporting information; Taylor et al., 2012) model experiments are used (see Table S1 for details). The historical (HIST) and Representative Concentration Pathway 8.5 (RCP8.5) experiments based on 37 CMIP5 atmosphere-ocean coupled models are used to represent the current (1962–2005) and future (2056–2099) climates. To investigate the physical mechanisms of the future changes of subtropical highs in the coupled models, several sets of AMIP (Atmospheric Model Intercomparison Project) experiments with prescribed SST from 11 out of the 37 atmosphere-only models are also used. The standard AMIP experiment is run with observed SSTs and sea ice and prescribed anthropogenic forcing. In addition, three AMIP experiments are also used to isolate the effects of CO_2 radiative forcing and SST warming. These include AMIP experiments with quadrupling of CO_2 forcing (AMIP4xCO2), uniform 4K SST warming (AMIP4K), and SST warming pattern derived from the coupled CMIP3 model experiments with a 1% per year increase in CO_2 at the time of CO_2 quadrupling (AMIPFuture). The differences between AMIP4xCO2 and AMIP are used to estimate the climate response to direct radiative forcing, while the differences between AMIP4K (AMIPFuture) and AMIP are used to estimate the climate response to uniform SST warming (SST warming pattern).

The NPSH is defined using the sea-level pressure averaged over Pacific (25–45°N, 180°E–130°W), and the NASH is defined similarly over Atlantic (25–45°N, 70–20°W). The zonal mean component of the NPSH and NASH is calculated as the zonal mean sea-level pressure averaged over the latitudinal band 25–45°N, while the zonally asymmetric component is calculated as the sea-level pressure anomalies with respect to the zonal mean. To compare with previous studies (Li et al., 2012; Shaw & Voigt, 2015), we also calculated the NPSH and NASH using the 925-hPa stream function in the same regions as the sea-level pressure. Following He et al. (2017), the Poisson equation $\nabla^2\psi = \xi$ is solved using the vorticity ξ to obtain the stream function ψ. The NPSH and NASH changes represented using the 925-hPa stream function display similar future changes to those defined by the sea-level pressure, with correlation coefficients of 0.83 and 0.92 for the seasonal difference between AMJ and JAS. As there are many missing values in the low-level (e.g., 925 hPa) wind field due to topography, we need to manually *fill* the missing values when we solve the equation. Hence, in later analysis, we only use the subtropical high index defined by the sea-level pressure.

To distinguish whether the subtropical high change is due to the intensity and/or location change, we calculate the centroid position of the NPSH and NASH in both the current and future climates. We define an intensity index of the subtropical high as the sea-level pressure average in a 10° by 10° box centered around the centroid of the subtropical high. This way, we obtain both the intensity and location changes by taking the difference between the future and current climates. To determine the regional implications of the subtropical high changes, we also analyze the Great Plains low-level jet (GPLLJ), which is defined using the 925-hPa meridional wind averaged over (26–38°N, 92–102°W). The agreement on the sign of the response from more than 70% of the multimodels is used to demonstrate the statistical robustness (He et al., 2017; Power et al., 2012). Our main results are not substantially influenced by using 75% or 80% as the thresholds.

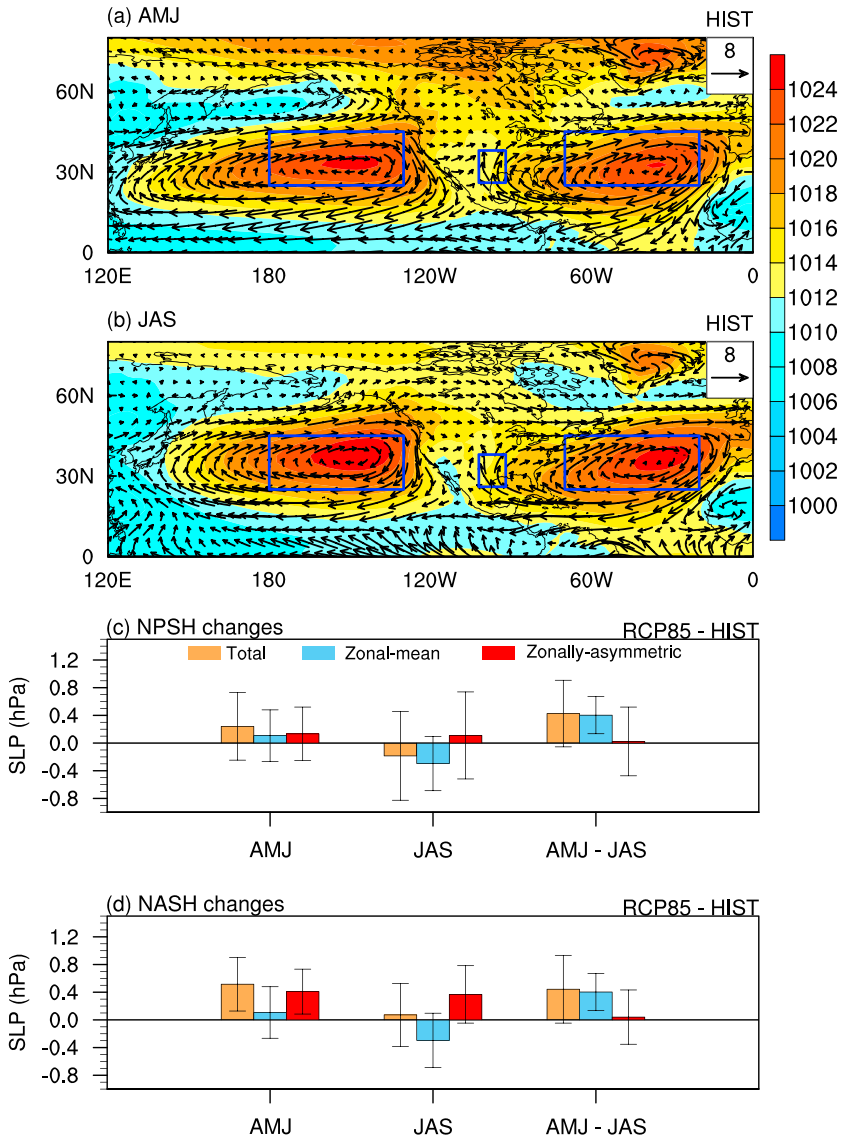

Figure 1. Climatology of the 925-hPa wind (vectors; unit: m/s) and sea-level pressure (shading; unit: hPa) during (a) April–June (AMJ) and (b) July–September (JAS) in the historical (HIST) experiment. The blue box shows where the North Pacific subtropical high (NPSH), North Atlantic subtropical high (NASH), and Great Plains low-level jet are defined. The changes of the (c) NPSH and (d) NASH between the RCP8.5 and HIST experiments during AMJ and JAS and the difference of AMJ minus JAS. The total change and its zonal mean and zonally asymmetric components are shown in orange, blue, and red bars, respectively. The error bar shows one standard deviation among the 37 models. RCP8.5 = Representative Concentration Pathway 8.5; SLP = sea-level pressure.

3. Results

3.1. Future Changes of the North Pacific and NASH

Figures 1a and 1b show the climatology of 925-hPa winds and sea-level pressure during boreal spring (AMJ) and summer (JAS). Both the NPSH and NASH are well structured with comparable magnitude between the two seasons. At the westward flank of the NASH, the GPLLJ is evident and plays an important role in transporting moisture from the Gulf of Mexico to the central and midwestern United States. Under global warming, the NPSH is moderately enhanced during spring, with almost equal contributions from the zonal mean and zonally asymmetric components for the multimodel ensemble mean (44.5% and 55.5%, respectively; Figure 1c). More specifically, 26 out of 37 models show a stronger NPSH under global warming during spring (Figure S1a). The enhancement of the NASH during spring is even more robust, with 35 out of 37 models

showing the same sign (Figure S1b). For the multimodel ensemble mean, the zonal mean component only contributes 20.8% to the enhancement of the NASH during spring, while the contribution from the zonally asymmetric component is 79.2%. As a regional manifestation of the NASH, the GPLLJ also becomes stronger during spring in all models (Figure S1c), consistent with the finding of Cook et al. (2009) based on CMIP3 models.

During summer, however, the responses of the NPSH and NASH are much weaker and less robust (Figures S1d and S1e): the NPSH is slightly weakened while the NASH is slightly strengthened based on the multimodel ensemble mean, but only 22 and 24 out of 37 models show the same sign as the multimodel ensemble mean for NPSH and NASH, respectively. As pointed out in previous studies (Kelly et al., 2018; Shaw & Voigt, 2015), the NASH mainly exhibits a westward shift under global warming during summer, which has been linked to the African and Indian monsoon heating (e.g., Kelly et al., 2018), while the NPSH involves a tug of war between radiative forcing and indirect SST warming, ending up with a weak and uncertain response (Shaw & Voigt, 2015). Decomposing the subtropical high change into zonal mean and zonally asymmetric components, we found that both the NPSH and NASH also involve another tug of war between the Hadley cell and land-sea contrast during summer: the Hadley cell tends to weaken the subtropical high, while the land-sea contrast strengthens it. As a result, they jointly produce a rather weak and uncertain response of the subtropical high during summer.

Comparing spring and summer, although the changes in the zonally asymmetric component are almost the same, the changes in the zonal mean component flip signs from spring to summer. This indicates that changes in the seasonal variation of land-sea contrast are much weaker compared to those due to the Hadley cell. Considering the seasonal difference, both the NPSH and NASH robustly strengthen more during spring relative to summer, with 31 and 30 out of 37 models showing the same sign, respectively (Figures S1f and S1g). These seasonally dependent responses are mainly attributable to the zonal mean component (94.5% and 90.9% for NPSH and NASH, respectively). As found in Song et al. (2018), there is a robust seasonally dependent response of the zonal mean component of the subtropical highs. Our results here demonstrate the dominant role of the zonal mean component in the robust seasonally dependent response of the NPSH and NASH, as manifested in larger enhancement during spring than summer. Our results do not change qualitatively if we define March-April-May as spring and June-July-August (JJA) as summer (Figure S2).

The seasonality changes of the subtropical high consist of both intensity and location components. Many previous studies (e.g., Kang & Lu, 2012; Lu et al., 2007; Tao et al., 2016) noted the poleward expansion of the descending branch of the Hadley cell under global warming, but whether the subtropical high expands northward following the Hadley cell is still unclear. As shown in Figure S3, both the NPSH and NASH are robustly enhanced more during spring than summer in intensity, with 29 and 28 models showing the same sign, although the intensity change in each month is not robust (left panel of Figure S3). Meanwhile, both the NPSH and NASH exhibit a robust poleward shift in each month during the warm season, and the NASH shifts poleward more during spring than summer (right panel of Figure S3). Hence, the subtropical high seasonality changes discussed above feature both intensity and location seasonality changes.

3.2. Relative Roles of Direct Radiative Forcing and Indirect SST Warming

The atmospheric response to global warming can be roughly attributed to two processes: one associated with direct radiative forcing and the other associated with indirect SST warming. Shaw and Voigt (2015) found that during the peak season (JJA), direct radiative forcing and indirect SST warming compete with each other by producing opposite responses of the NPSH, while they work collaboratively for the NASH. Here we find that both the NPSH and NASH have a robust seasonally dependent response, and they are robustly enhanced during spring relative to summer. To distinguish the relative roles of direct radiative forcing and indirect SST warming on the robust responses, we plot the responses of the sea-level pressure and low-level winds under different forcing scenarios during AMJ and the interseasonal difference of AMJ minus JAS in Figure 2. During AMJ, the most evident high-pressure and anticyclonic circulation anomalies occur over the North Atlantic, while the northern Eurasian continent is occupied by significant low pressure and cyclonic circulation anomalies (Figure 2a). The high-pressure and anticyclonic circulation anomalies are contributed by both direct radiative forcing (Figure 2c) and indirect SST warming (Figure 2e, g), while the low-pressure and cyclonic circulation anomalies are mainly contributed by direct radiative forcing, which is canceled to

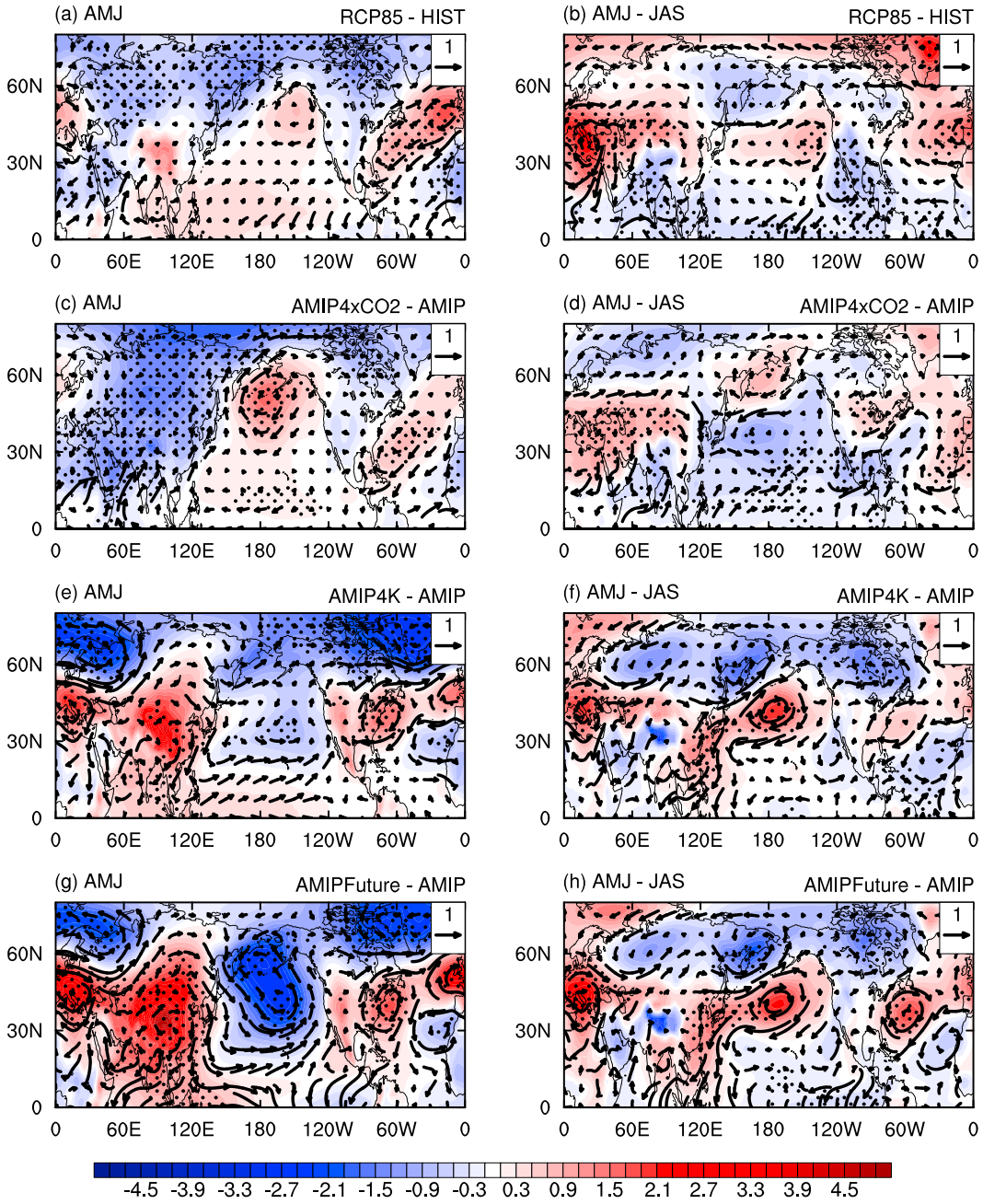

Figure 2. Sea-level pressure (shading; unit: hPa) and 925-hPa wind (vectors; unit: m/s) changes during (left column) AMJ and (right column) AMJ minus JAS for (a and b) RCP8.5 minus HIST, (c and d) AMIP4xCO2 minus AMIP, (e and f) AMIP4K minus AMIP, and (g and h) AMIPFuture minus AMIP. Stippling indicates that at least 70% of the models agree on the sign of the difference. AMJ = April–June; JAS = July–September; RCP8.5 = Representative Concentration Pathway 8.5; AMIP = Atmospheric Model Intercomparison Project; HIST = historical.

some extent by the contribution from SST warming. The high-pressure anomalies over the western Pacific (Figure 2a) indicate the weakening of Walker circulation under global warming and are mainly due to the El Niño-like SST warming (Figures 2e and 2g), consistent with many previous studies (e.g., Held & Soden, 2006; Vecchi & Soden 2007; Yang et al., 2016). When considering the seasonal difference (Figure 2b), besides the stronger NPSH and NASH changes during AMJ than JAS, the high-pressure and anticyclonic circulation anomalies extending from North Atlantic to the Eurasia continent form a quasi-zonal high-pressure band over the northern subtropics. Direct radiative forcing has a significant contribution to the high-pressure and anticyclonic circulation anomalies over the Mediterranean and Middle East (Figure 2d),

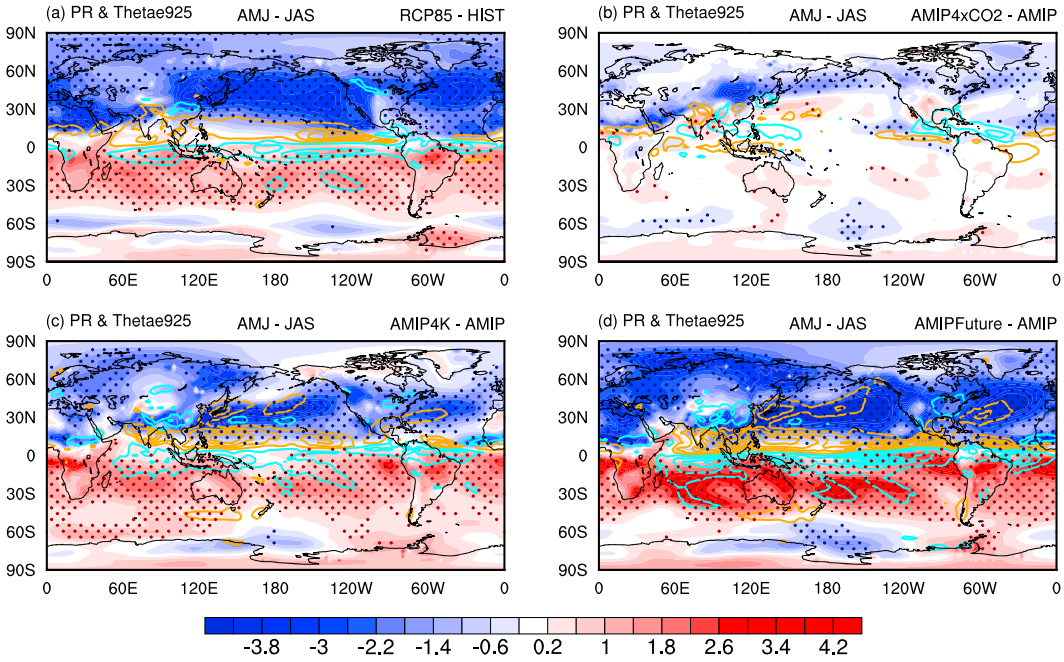

Figure 3. Seasonal differences of precipitation (contours; unit: mm/day) and 925-hPa equivalent potential temperature θ_e (shading; unit: K) between AMJ and JAS for (a) RCP8.5 minus HIST, (b) AMIP4xCO2 minus AMIP, (c) AMIP4K minus AMIP, and (d) AMIPFuture minus AMIP. The cyan and orange contours on the left panels indicate positive and negative precipitation anomalies, respectively. The contour interval is 1 mm/day with the first positive and negative contours corresponding to 0.5 and −0.5 mm/day, respectively. Stippling indicates that at least 70% of the models agree on the sign of the θ_e difference. AMJ = April–June; JAS = July–September; RCP8.5 = Representative Concentration Pathway 8.5; AMIP = Atmospheric Model Intercomparison Project; HIST = historical.

while indirect SST warming not only contributes to the high-pressure anomalies over the Mediterranean but also dominates the seasonally dependent response of the NPSH and NASH (Figures 2f and 2h).

During spring, we can see clear opposite effects between direct radiative forcing and SST warming on the sea level pressure and circulation over North Pacific and East Asia (left column of Figure 2), similar to the tug-of-war relationship suggested by Shaw and Voigt (2015) for JJA. However, the sum of direct radiative forcing and indirect SST warming is not consistent with the total response in the coupled models over the North Pacific and East Asia but roughly consistent over the North Atlantic region (Figures S4a and S4c). For the interseasonal difference, the sum of the individual response and the total responses correspond with each other quite well (Figures S4b and S4d). As also mentioned by Biasutti (2013), decomposition of the coupled response to direct radiative forcing and indirect SST warming components may not work quantitatively at regional scale. Hence, we caution the use of direct radiative forcing and indirect SST warming for understanding the coupled response over the North Pacific and East Asia during spring.

3.3. Mechanisms Responsible for the Enhancement During Spring and the Seasonally Dependent Responses of the NPSH and NASH

The zonal mean component of subtropical highs corresponds to the descending branch of the Hadley cell, while the zonally asymmetric component is associated with land-sea thermal contrast. According to the theory of the Hadley cell (Lindzen & Hou 1988), off-equator diabatic heating has asymmetric effects on the strength of the Hadley cell in the two hemispheres: when the diabatic heating is located north of the equator, the northern Hadley cell is weakened and the southern Hadley cell is intensified, and vice versa. As shown in Figure S5, during AMJ, a first glance suggests that tropical precipitation increases mainly along the equator (Figure S5a), contributed mostly by SST warming (Figures S5c and S5d). This is because climatological precipitation during this season lies along the equator, and the *wet-get-wetter* mechanism plays a very important role under global warming (Held & Soden, 2006; Huang et al., 2013). However, as discovered by Biasutti and Sobel (2009) based on CMIP3 models and confirmed by Song et al. (2018) from CMIP5 models, there is a significant seasonal delay in tropical precipitation under warming, which means that during the transitional season of AMJ, precipitation in the southern tropics will still be larger than precipitation in the northern tropics in

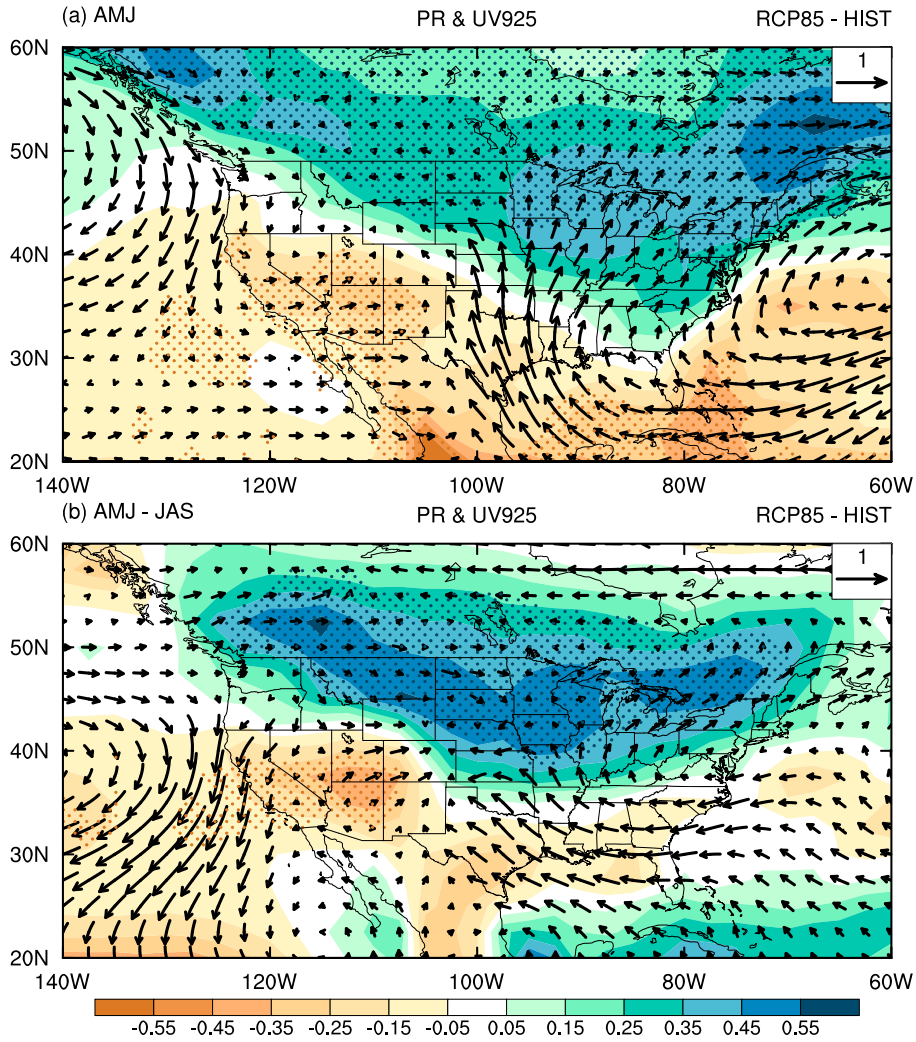

Figure 4. Changes of the 925-hPa wind (vector; unit: m/s) and precipitation (shading; unit: mm/day) during (a) AMJ and (b) AMJ minus JAS for RCP8.5 minus HIST. Stippling indicates that at least 70% of the models agree on the sign of the difference. AMJ = April–June; JAS = July–September; RCP8.5 = Representative Concentration Pathway 8.5; HIST = historical.

the future (see Figure 2 in Song et al. (2018)). As such, the total tropical rain belt and the associated latent heating shift toward south of the equator and the northern Hadley cell will be enhanced during AMJ under global warming, consistent with the enhanced zonal mean component (Figures 1c and 1d).

For the zonally asymmetric component during AMJ, the response is related to land-sea thermal contrast, as suggested in many previous studies (Li et al., 2012; Shaw & Voigt, 2015). As shown in Figures S5 and S6, the low-level equivalent potential temperature θ_e displays an enhanced contrast not only between East Asia and North Pacific but also between North America and North Atlantic, favoring the zonally asymmetric component of the subtropical highs. Both direct radiative forcing and indirect SST warming contribute to the enhanced θ_e contrast, which is consistent with the zonally asymmetric subtropical high response under these two forcings (Figures 1c and 1d).

For the interseasonal difference between AMJ and JAS, θ_e features a north-south contrast, with negative (positive) θ_e interseasonal difference in the Northern (Southern) Hemisphere, but there is no clear land-sea contrast (Figure 3a). The north-south θ_e contrast is consistent with the interhemispheric energy contrast between the two seasons revealed by Song et al. (2018). The weak land-sea θ_e contrast is consistent with the small interseasonal difference in the response of the zonally asymmetric component of subtropical highs shown in Figures 1c and 1d. The interhemispheric θ_e contrast is produced by both uniform SST warming and

SST warming pattern forcings (Figures 3c and 3d) but not by direct radiative forcing (Figure 3b). Consistent with the interhemispheric θ_e contrast, precipitation also features a dipole pattern in the tropics, with negative (positive) precipitation over the northern (southern) tropics. It should be pointed out that during JAS, the climatological precipitation band is located in the northern tropics, so the enhanced amplitude of precipitation due to increased moisture in a warming world via the wet-get-wetter mechanism (Held & Soden, 2006; Huang et al., 2013) also has a substantial contribution to the interseasonal north-south dipole pattern of precipitation. Hence, the interseasonal dipole pattern of precipitation includes two parts: one is due to the seasonal delay of precipitation during spring, and the other is the amplified precipitation band during summer. This dipole pattern of precipitation and the associated diabatic heating drives an enhancement of the Northern Hemisphere Hadley cell and a weakening of the Southern Hemisphere Hadley cell as suggested by Song et al. (2018), consistent with the enhanced zonal mean component of the NPSH and NASH.

3.4. Implications for the U.S. Regional Climate

The robust enhancement of the NASH and NPSH during spring and their seasonally dependent responses have great implications for the U.S. regional climate, as these two systems are located just west and east of the contiguous United States, respectively. Figure 4 shows the precipitation and 925-hPa winds over the United States during AMJ and the interseasonal difference of AMJ minus JAS. During AMJ, due to the enhanced GPLLJ, enhancement and northward shift of the NASH, and increased moisture with warming, precipitation is enhanced over the northern Great Plains and northeastern United States due to increased moisture transport (Figure 4a). Meanwhile, precipitation is increased (decreased) over northwestern (southwestern) United States due to the enhanced and northward shift of the NPSH and increased moisture, as the enhanced westerly in the poleward flank of the NPSH transports more moisture to the northwestern United States, but the enhanced northerly wind in the eastern flank of the NPSH diverges more moisture away from the southwestern United States. The seasonal difference between AMJ and JAS shows a similar pattern to that during AMJ, suggesting that the AMJ response dominates the seasonally dependent response over the United States (Figure 4b). As moisture transport by the GPLLJ is also important for mesoscale convective systems in the central and midwestern United States (Feng et al., 2016; Wang & Chen, 2009), the robust enhancement of the GPLLJ during AMJ may provide an important constraint for projecting possible future changes of mesoscale convective systems and the extreme precipitation they might bring.

4. Conclusions

In this study, future changes of the NPSH and NASH during the warm season are investigated based on the historical and RCP8.5 experiments from 37 CMIP5 models. It is found that both the NPSH and NASH are consistently enhanced more during spring than summer, consistent with the seasonally dependent response of the zonal mean component of the subtropical highs elucidated by Song et al. (2018). Decomposing the total response of the subtropical highs into zonal mean and zonally asymmetric components, we found that the zonal mean component dominates the seasonally dependent responses of the NPSH and NASH (94.5% and 90.9%, respectively), while the zonally asymmetric component contributes 55.5% and 79.2% to the robustly enhanced NPSH and NASH during spring, respectively.

The zonal mean component is related to the descending branch of the Hadley cell, while the zonally asymmetric component is related to land-sea thermal contrast. For the interseasonal difference of the response between spring and summer (AMJ-JAS), precipitation over the northern (southern) tropics decreases (increases), forming a zonally elongated dipole pattern. This dipole precipitation pattern enhances the Hadley cell in the Northern Hemisphere, so the zonal mean component of the NPSH and NASH is also enhanced due to the stronger descending branch. Meanwhile, low-level θ_e features an obvious interhemispheric contrast but no clear land-sea contrast, so the zonally asymmetric components of the NPSH and NASH play a relatively minor role in the interseasonal difference of the subtropical highs. But for AMJ, land-sea thermal contrast is much stronger under global warming and the zonally asymmetric component plays a major role. The enhanced NPSH and NASH during AMJ can be attributed to both direct radiative forcing and indirect SST warming through changing land-sea thermal contrast, while the seasonally dependent response of the NPSH and NASH is mainly due to indirect SST warming through the Hadley cell response.

The two aspects of the robust future changes of the NPSH and NASH have important implications for the U.S. regional climate. Due to the increased moisture transport, along with the enhanced NPSH and GPLLJ,

northeastern regions of the United States will become wetter during AMJ, while the southwestern regions will become drier. The winter and summer precipitation changes in the southwestern United States have been discussed previously by Seager et al. (2007) and Seager and Vecchi (2010), highlighting an overall drying trend in the future. Gao et al. (2014) noted the robust spring drying in the southwestern United States and the seasonal migration of wet/dry patterns under global warming. Here the robust spring drying is found to be caused by the enhanced NPSH during spring due to the combined contributions from the land-sea contrast and the Hadley cell. The contrast in spring versus summer precipitation response to warming may have important implications for agriculture and water resources in the United States through changes in planting dates and hydrologic regimes. Similarly, strengthening of the NPSH during spring also has a noticeable influence on precipitation in East Asia (Figure 3a). As the NPSH is only one of the circulation features transporting moisture for the East Asian monsoon precipitation, more analysis is being pursued to explore the relationships among the Hadley cell, the subtropical highs, and the seasonality of subtropical monsoon rainfall.

Acknowledgments
This research is supported by the U.S. Department of Energy Office of Science Biological and Environmental Research as part of the Regional and Global Climate Modeling program and Multi-sector Dynamics program. PNNL is operated for the Department of Energy by Battelle Memorial Institute under contract DE-AC05-76RL01830. We acknowledge the World Climate Research Program's Working Group on Coupled Modeling, which is responsible for CMIP, and thank the climate modeling groups (listed in supporting information Table S1) for producing and making available their model output. For CMIP, the U.S. DOE's Program for Climate Model Diagnosis and Intercomparison (PCMDI) provides coordinating support and led development of software infrastructure in partnership with the Global Organization for Earth System Science Portals.

References

Biasutti, M. (2013). Forced Sahel rainfall trends in the CMIP5 archive. *Journal of Geophysical Research: Atmospheres*, *118*, 1613–1623. https://doi.org/10.1002/jgrd.50206

Biasutti, M., & Sobel, A. H. (2009). Delayed Sahel rainfall and global seasonal cycle in a warmer climate. *Geophysical Research Letters*, *36*, L23707. https://doi.org/10.1029/2009GL041303

Chang, C.-P., Zhang, Y., & Li, T. (2000). Interannual and interdecadal variations of the East Asian summer monsoon and tropical Pacific SSTs. Part I: Roles of the subtropical ridge. *Journal of Climate*, *13*, 4310–4325.

Colbert, A., & Soden, B. (2012). Climatological variations in North Atlantic tropical cyclone tracks. *Journal of Climate*, *25*(2), 657–673. https://doi.org/10.1175/JCLI-D-11-00034.1

Cook, K. H., Vizy, E. K., Launer, Z. S., & Patricola, C. M. (2009). Springtime intensification of the Great Plains low-level jet and Midwest precipitation in GCM simulations of the twenty-first century. *Journal. Climacteric*, *21*, 6321–6340.

Feng, Z., Leung, L. R., Hagos, S., Houze, R. A., Burleyson, C. D., & Balaguru, K. (2016). More frequent intense and long-lived storms dominate the springtime trend in central US rainfall. *Nature Communications*, *7*, 13429. https://doi.org/10.1038/ncomms13429

Gao, Y., Leung, L. R., Lu, J., Liu, Y., Huang, M., & Qian, Y. (2014). Robust spring drying in the southwestern U.S. and seasonal migration of wet/dry patterns in a warmer climate. *Geophysical Research Letters*, *41*, 1745–1751. https://doi.org/10.1002/2014GL059562

He, C., Wu, B., Zou, L., & Zhou, T. (2017). Responses of the summertime subtropical anticyclone to global warming. *Journal of Climate*, *30*(16), 6465–6479. https://doi.org/10.1175/JCLI-D-16-0529.1

Held, I. M., & Soden, B. J. (2006). Robust responses of the hydrological cycle to global warming. *Journal of Climate*, *19*(21), 5686–5699. https://doi.org/10.1175/JCLI3990.1

Hoskins, B. J. (1996). On the existence and intensity of summer subtropical anticyclones. *Bulletin of the American Meteorological Society*, *77*, 1287–1291.

Huang, P., Xie, S. P., Hu, K. M., Huang, G., & Huang, R. H. (2013). Patterns of the seasonal response of tropical rainfall to global warming. *Nature Geoscience*, *6*(5), 357–361. https://doi.org/10.1038/ngeo1792

Kang, S. M., & Lu, J. (2012). Expansion of the Hadley cell under global warming: Winter versus summer. *Journal of Climate*, *25*(24), 8387–8393. https://doi.org/10.1175/JCLI-D-12-00323.1

Kelly, P., Kravitz, B., Lu, J., & Leung, L. R. (2018). Remote drying in the North Atlantic as a common response to precessional changes and CO_2 increase over land. *Geophysical Research Letters*, *45*, 3615–3624. https://doi.org/10.1002/2017GL076669

Li, W., Li, L., Fu, R., Deng, Y., & Wang, H. (2011). Changes to the North Atlantic subtropical high and its role in the intensification of summer rainfall variability in the southeastern United States. *Journal of Climate*, *24*(5), 1499–1506. https://doi.org/10.1175/2010JCLI3829.1

Li, W., Li, L., Ting, M., & Liu, Y. (2012). Intensification of Northern Hemisphere subtropical highs in a warming climate. *Nature Geoscience*, *5*, 830–834.

Lindzen, R. S., & Hou, A. Y. (1988). Hadley circulations for zonally averaged heating centered off the equator. *Journal of the Atmospheric Sciences*, *45*, 2417–2427.

Lu, J., Vecchi, G. A., & Reichler, T. (2007). Expansion of the Hadley cell under global warming. *Geophysical Research Letters*, *34*, L06805. https://doi.org/10.1029/2006GL028443

Namias, J. (1972). Influence of Northern Hemisphere general circulation on drought in northeast Brazil. *Tellus*, *24*, 336–343.

Power, S. B., Delage, F., Colman, R., & Moise, A. (2012). Consensus on twenty-first-century rainfall projections in climate models more widespread than previously thought. *Journal of Climate*, *25*(11), 3792–3809. https://doi.org/10.1175/JCLI-D-11-00354.1

Rodwell, M. J., & Hoskins, B. J. (2001). Subtropical anticyclones and summer monsoon. *Journal of Climate*, *14*(15), 3192–3211. https://doi.org/10.1175/1520-0442(2001)014<3192:SAASM>2.0.CO;2

Seager, R., Ting, M., Held, I., Kushnir, Y., Lu, J., Vecchi, G., et al. (2007). Model projections of an imminent transition to a more arid climate in southwestern North America. *Science*, *316*(5828), 1181–1184. https://doi.org/10.1126/science.1139601

Seager, R., & Vecchi, G. A. (2010). Greenhouse warming and the 21st century hydroclimate of southwestern North America. *Proceedings of the National Academy of Sciences*, *107*(50), 21,277–21,282. https://doi.org/10.1073/pnas.0910856107

Shaw, T. A., & Voigt, A. (2015). Tug of war on the summertime circulation between radiative forcing and sea surface warming. *Nature Geoscience*, *8*(7), 560–566. https://doi.org/10.1038/ngeo2449

Song, F., Leung, L. R., Lu, J., & Dong, L. (2018). Seasonally-dependent responses of subtropical highs and tropical rainfall to anthropogenic warming. *Nature Climate Change*, *8*(9), 787–792. https://doi.org/10.1038/s41558-018-0244-4

Stowasser, M., Wang, Y., & Hamilton, K. (2007). Tropical cyclone changes in the western North Pacific in a global warming scenario. *Journal of Climate*, *20*(11), 2378–2396. https://doi.org/10.1175/JCLI4126.1

Tao, L., Hu, Y., & Liu, J. (2016). Anthropogenic forcing on the Hadley circulation in CMIP5 simulations. *Climate Dynamics*, *46*(9-10), 3337–3350. https://doi.org/10.1007/s00382-015-2772-1

Taylor, K. E., Stouffer, R. J., & Meehl, G. A. (2012). An overview of CMIP5 and the experiment design. *Bulletin of the American Meteorological Society*, *93*(4), 485–498. https://doi.org/10.1175/BAMS-D-11-00094.1

Vecchi, G. A., & Soden, B. J. (2007). Global warming and the weakening of the tropical circulation. *Journal of Climate*, *20*(17), 4316–4340.

Wang, B., Xiang, B., & Lee, J.-Y. (2013). Northern Hemisphere summer monsoon intensified by mega-El Niño/southern oscillation and Atlantic multidecadal oscillation. *Proceedings of the National Academy of Sciences of the United States of America*, *110*(14), 5347–5352. https://doi.org/10.1073/pnas.1219405110

Wang, S.-Y., & Chen, T. (2009). The late-spring maximum of rainfall over the U.S. central plains and the role of the low-level jet. *Journal of Climate*, *22*(17), 4696–4709. https://doi.org/10.1175/2009JCLI2719.1

Wu, L., Wang, B., & Geng, S. (2005). Growing typhoon influence on East Asia. *Geophysical Research Letters*, *32*, L18703. https://doi.org/10.1029/2005GL022937

Yang, J., Peltier, W. R., & Hu, Y. (2016). Monotonic decrease of the zonal SST gradient of the equatorial Pacific as a function of CO_2 concentration in CCSM3 and CCSM4. *Journal of Geophysical Research: Atmospheres*, *121*, 10,637–10,653. https://doi.org/10.1002/2016JD025231

Zhou, T., & Yu, R. (2005). Atmospheric water vapor transport associated with typical anomalous summer rainfall patterns in China. *Journal of Geophysical Research*, *110*, D08104. https://doi.org/10.1029/2004JD005413